Appl Phys A (2012) 108:29–34
DOI 10.1007/s00339-012-6964-9

Applied Physics A
Materials Science & Processing

RAPID COMMUNICATION

3D grafting via three-photon induced photolysis of aromatic azides

A. Ovsianikov · Z. Li · A. Ajami · J. Torgersen · W. Husinsky · J. Stampfl · R. Liska

Received: 14 February 2012 / Accepted: 1 May 2012 / Published online: 13 May 2012

Abstract Utilization of multiphoton absorption has led to important advances in microscopy and photofabrication. Herein, our recent results on precise immobilization of molecules within 3D polymeric matrices by means of multiphoton grafting are presented. Assessment of nonlinear absorption properties of difunctional aromatic azide, selected for this purpose was performed by the Z-scan technique. It indicates that a three-photon absorption process is responsible for photolysis of this compound. Successful photografting for production of 3D patterns with lateral resolution down to 4 μm was achieved. Our results demonstrate the potential of the developed three-photon grafting method for precise 3D site-specific functionalization of different materials.

1 Introduction

Photografting is a method for modification of material surfaces through light-initiated covalent binding of functional molecules. Azides and their derivatives are often used for photografting due to their high photosensitivity [1]. The fact that the nitrene, produced upon photolysis, are immobilized via insertion reaction into CH or NH bonds provides their applicability to a wide variety of polymeric matrices. UV grafting of aromatic azide derivatives was reported for modification of glassy carbon surfaces [2], preparation of poly(ethylene glycol) (PEG) brushes on polysulfone membranes [3], functionalization of membranes [4], and even for RNA-protein crosslinking [5]. By using multiphoton absorption for the initiation it is possible to immobilize different molecules with even higher precision, since the light-material interaction occurs only in a confined area within the focal spot. In addition to a more accurate functionalization, true 3D patterns can be produced using this approach. The capabilities of multi-photon absorption-based direct laser writing are well illustrated in the reports on two-photon polymerization [6–9]. Few related studies addressed the question of highly active photoinitiators, exhibiting large multiphoton absorption cross-sections. It is known from the area of two-photon polymerization that highly effective chromophores are characterized by a planar conjugated system containing donor and acceptor groups [10, 11].

Herein, we describe the first attempt to combine classical azide grafting reactions with multiphoton photochemistry. The 2,6-bis(4-azidobenzylidene)-4-methylcyclohexanone (BAC-M) was selected for the multiphoton grafting experiments based on criteria known from two-photon polymerization. By using the Z-scan technique, the order of the nonlinear absorption process and also the multiphoton absorption cross section of the utilized aromatic azide were determined. Demonstrated laser photografting of BAC-M within a PEG-based matrix provides a proof of the concept for the selective molecule immobilization in 3D. Its potential applications are configurable systems for studies of cell-matrix

A. Ovsianikov (✉) · J. Stampfl
Institut für Werkstoffwissenschaft und Werkstofftechnologie, Technische Universität Wien, Wien, 1040, Austria
e-mail: Aleksandr.Ovsianikov@tuwien.ac.at

Z. Li · J. Torgersen · R. Liska
Institut für Angewandte Synthesechemie, Technische Universität Wien, Wien, 1060, Austria

R. Liska
e-mail: rliska@ioc.tuwien.ac.at

A. Ajami · W. Husinsky
Institut für Angewandte Physik, Technische Universität Wien, Wien, 1040, Austria

interactions, sensing applications, microarrays for proteome analysis and drug screening.

2 Material and methods

2.1 Spectroscopic and Z-scan material characterization

The UV-Vis absorption spectra of BAC-M with a concentration of 1.0×10^{-5} mol L^{-1} in acetonitrile were recorded on a Hitachi U-2001 spectrometer. For the evaluation of the order of the multiphoton process and the absorption cross-section the Z-scan technique was employed [12]. This technique involves the sample scanning along the beam propagation direction (z-axis) through the focal plane of a focused laser beam. As the sample approaches the focal plane, the nonlinear absorption increases due to its dependence on the intensity of light. The two-photon absorption (2PA) probability is proportional to the square of light intensity; the three-photon absorption (3PA) is proportional to the third order of light intensity and so on. The light transmitted through the sample is collected using a large diameter convex lens and then directed to a detector. The scanning result is a symmetric V-shaped signal showing higher absorption at the focal plane and less absorption at the sample position away from the focus. The order of nonlinear absorption can be determined fitting the theoretical equations for different order of nonlinear absorption to the experimental Z-scan data. From the fitting process, in addition to the nonlinear absorption coefficient, the value of the Rayleigh length can be extracted. If the appropriate equation is fitted to the experimental Z-scan data, this extracted Rayleigh length value should match the value measured experimentally. In this way, the Z-scan technique provides a way to determine the order of nonlinearity. After determining the order of nonlinear absorption, the multiphoton absorption cross-section can be extracted from the fitting of the respective equation to the experimental Z-scan data. Assuming that 2PA is the predominant nonlinear absorption process the theoretical equation is given as [12]:

$$T(z) = \sum_{n=0}^{\infty} \frac{(-q_0)^n}{(n+1)^{3/2}(1+x^2)^n} \tag{1}$$

where $q_0 = N_A \rho \times 10^{-3} L I_0 \sigma_2 \lambda / hc$, N_A is the Avogadro number, ρ is the concentration, L is the thickness of the sample, I_0 is the maximum on axis intensity at the focus, which is calculated from $I_0 = 4\sqrt{\ln 2/\pi}\, E_p/(\pi w_0^2 \tau)$ (E_p is the pulse energy, w_0 is the beam waist radius, and τ is the pulse duration), λ is the wavelength of the laser radiation, σ_2 is the 2PA cross-section, h is the Planck constant, c is the speed of light in free space, x is a unitless variable defined as z/z_0, z is the sample position measured with respect to the focal point and z_0 is the Rayleigh length.

If the 3PA is the predominant nonlinear absorption process the theoretical equation is [14, 15]:

$$T(z) = \sum_{m=0}^{\infty} \frac{(-P_0^2)^m}{(2m)!(2m+1)^{3/2}(x^2+1)^{2m}} \tag{2}$$

where

$$P_0^2 = 2N_A \rho \cdot 10^{-3} L I_0^2 \sigma_3 \lambda^2 / (hc)^2 \tag{3}$$

and, σ_3 is the 3PA cross section.

An amplified laser system (FemtoPro, Femtolaser) delivering 100 fs pulses at a repetition rate of 1 kHz at 795 nm was used for the Z-scan experiments. A 0.2 mm thick cell filled with BAC-M solution was mounted on a translating stage, which can move the sample for a distance of 24 mm through the focus. The computer software analyzes the intensity of individual laser pulses (including averaging over several laser shots) and also handles the movement of the translation stage as well as the entire data acquisition process.

The Rayleigh length for our set up was measured to be 0.82 mm which is compatible with the value calculated from $Z_0 = M^2 \lambda f^2 / \pi W^2$ in which the beam quality factor M^2 is 2, the focal length of the focusing lens f is 300 mm and the beam radius on the focusing lens W is 7.5 mm. The Rayleigh length in this experiment is four times larger than the thickness of the sample, which fulfills the thin sample condition. The average transmittance over 1,000 laser pulses was measured in each position in order to minimize the errors arising from the laser pulse energy fluctuations.

2.2 Laser grafting via three-photon absorption (3PA)

The samples (diameter 6 mm; thickness 1 mm) are prepared from poly(ethylene glycol) diacrylate (PEGDa, average Mn = 700 g/mol, Sigma Aldrich) containing 1 wt.% of photoinitiator Irgacure 2959 (Ciba SC) by photopolymerization with UV light for 5 minutes (Intelliray 600) in silicone molds. Photopolymerized material pellets are soaked in 50 % EtOH solution in order to remove residual monomer and photoinitiator. Next, the EtOH is replaced with DMF and the samples are stored until used.

For laser photografting the samples were immersed into the 2 wt% solution of 2,6-bis(4-azidobenzylidene)-4-methylcyclohexanone (BAC-M) in DMF (Fig. 3a). A Ti:sapphire femtosecond laser (High Q, Femtotrain) emitting pulses with duration of 80 fs at a repetition rate of 73 MHz around 793 nm was used. The laser beam was focused with a 20x microscope objective (Zeiss, NA = 0.4) into the samples. In order to verify a possibility of 3D photografting, a series of woodpile patterns were produced at a scanning velocity of 200 μm/s with an average laser power values in the range of 280–400 mW. A woodpile consists of

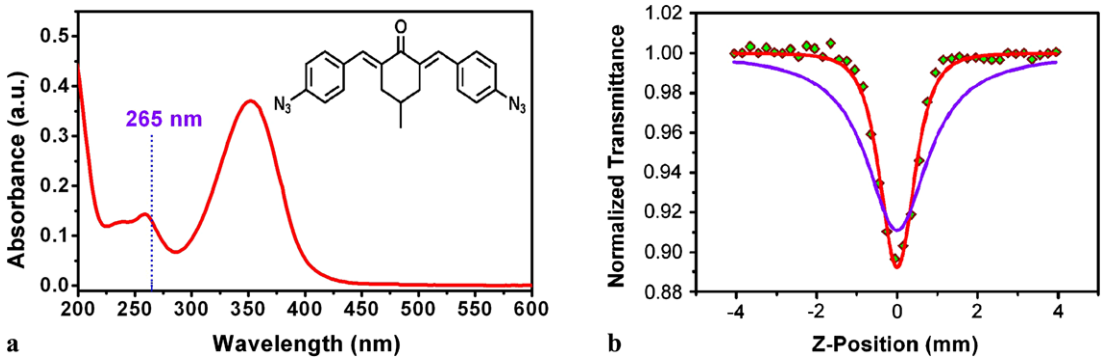

Fig. 1 (**a**) UV-Vis absorption spectra of the BAC-M. The *inset* shows the structure of BAC-M; (**b**) Results of the Z-scan characterization of BAC-M solution. *Red solid line* is the fit curve assuming the 3PA process and *blue solid line* is the fit curve assuming 2PA

layers of parallel lines, where each line is produced by a single laser scan at a distance "d" to each other. The stacking sequence repeats itself every four layers, while the adjacent layers are rotated by 90° and are produced at a distance of 5 µm. Between every other layer, the rods are shifted relative to each other by "$d/2$." The patterns are obtained by moving the sample position relatively to the laser focus in 3D using three linear translation stages in a layer-by-layer fashion. Immediately after the grafting procedure the samples was placed in DMF in order to remove residual BAC-M. Fluorescence of sample patterns was analyzed by laser scanning microscope (LSM700, ZEN software, Carl-Zeiss), at the excitation wavelength of 488 nm.

3 Results and discussion

The efficiency of 3D grafting process depends on the nonlinear absorption probability. In analogy to two photon polymerization, where highly sensitive photoinitiators are characterized by a planar conjugated system containing donor and acceptor groups [8, 10], BAC-M is expected to be an efficient multiphoton absorber. Figure 1a depicts the chemical structure and the UV−Vis absorption spectra of BAC-M. The evaluated compound does not exhibit any linear absorption beyond 430 nm and is completely transparent in the near infrared range. A weak absorption around 400 nm could allow the possibility of 2PA. However, it is unlikely for the 2PA to be the predominant nonlinear absorption process since the 2PA peak generally appears at a wavelength shorter than two times the linear absorption peak [16]. It is worth to mention that the probability of 3PA is orders of magnitude lower than that of 2PA. Thus, considerably higher intensities are required for 3PA to dominate. Since at high irradiation the 2PA in this compound might compete with 3PA, we first determined the order of the predominant nonlinear absorption. For this purpose, an open aperture Z-scan experiment was performed.

Figure 1b shows the results of a Z-scan measurement for BAC-M using 100 fs pulses with an energy of 160 nJ. The green solid line shows the fit curve using Eq. (1) assuming the 2PA process whereas, the red solid line shows the fit curve using Eq. (2) assuming the 3PA. In both fitting processes, the Rayleigh length is fixed to 0.82 mm as measured experimentally. Comparing these two fit curves clearly indicates that 3PA occurs in BAC-M.

In order to verify that our conclusion in determining the order of nonlinearity for BAC-M was accurate the Eq. (2) was fitted to the Z-scan data for different pulse energies as shown in Fig. 2a. From each fitting curve, the value of the variable P_0^2 was extracted.

According to the relation $P_0^2 = 2N_A\rho \cdot 10^{-3} L I_0^2 \sigma_3 \lambda^2 / (hc)^2$, the P_0^2 should scale linearly with intensity square (E_p^2) in case of a 3PA process. The values of P_0^2 extracted from fit curves in Fig. 2a are plotted versus E_p^2 in Fig. 2b. The solid red line represents a best fit curve resulting from the linear $P_0^2 = 2N_A\rho \cdot 10^{-3} L I_0^2 \sigma_3 \lambda^2/(hc)^2$. This linear behavior provides an additional proof, for the fact that the 3PA is indeed the predominant nonlinear absorption in BAC-M. From the best fit curve in Fig. 2b a value of 1.19×10^{-78} cm^6 s^2 was obtained for the 3PA cross-section of BAC-M. The obtained values are very close to those recently reported for a similar compound by Gu et al. [13].

It is important to mention that this is not the sole parameter defining the efficiency of the photografting process. Compounds with similar absorption cross-sections might still differ in their efficiency to produce reactive species.

Figure 3 shows the laser photografting strategy investigated in this work. The produced PEG-matrix swells in DMF, providing homogeneous distribution of BAC-M within it. The short-lived nitrene intermediate, generated by photolysis upon laser irradiation, directly attaches on the PEG network via insertion reaction (Fig. 3b). Such molecule immobilization process can be employed with any matrix containing C–H or N–H bonds. Compared to a popular chain-growth polymerization grafting, single-molecule in-

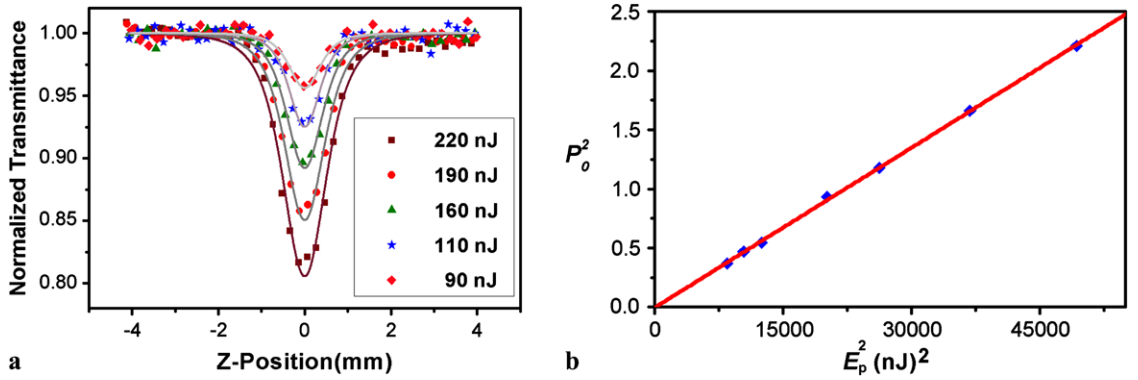

Fig. 2 Measured Z-scans of BAC-M for different pulse energies: (**a**) The *solid lines* are the fit curves assuming 3PA; (**b**) P_0^2 is plotted versus E_p^2

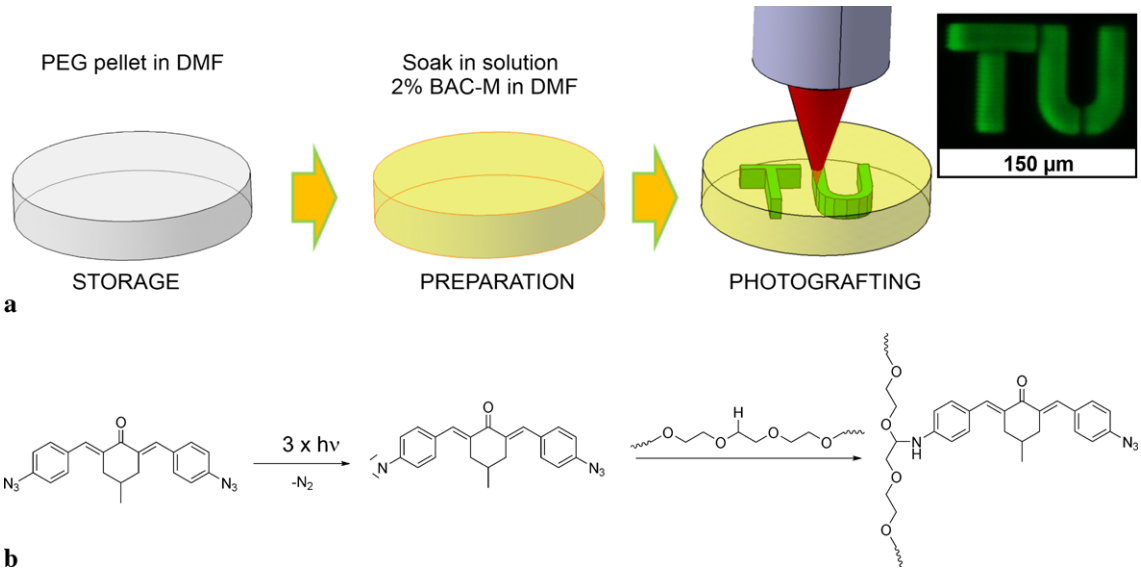

Fig. 3 Schematic principle of three-photon grafting: (**a**) sample preparation and processing; An *inset* shows a fluorescence microscope image of a Vienna University of Technology logo produced by three-photon grafting. (**b**) three-photon absorption (3PA) induced photolysis of BAC-M and its insertion into the PEG matrix

sertion mechanism, utilized here, potentially provides better control over the density of immobilized molecules.

After grafting and removal of the nonreacted azide, the main final photolytic product ketocyanine dye exhibits strong fluorescence [15]. Therefore, the produced patterns can be observed with laser scanning microscopy (LSM) directly after the grafting procedure, in contrast to previously reported methods requiring some additional fluorescence dye-bounding acrylate monomers in the presence of suitable photoinitators for characterization [17].

A series of woodpile patterns were produced at a scanning velocity of 200 µm/s with an average laser power values in the range of 20–400 mW. The patterns are obtained by moving the sample position relatively to the laser focus in 3D using three linear translation stages in a layer-by-layer fashion. An LSM image of an array of woodpile patterns is shown in Fig. 4a. The produced woodpile patterns have a size of 150 µm × 150 µm at line distance of 5 µm, 15 µm, and 25 µm. By varying the distance between the neighboring laser scans, one can switch from the woodpile patterns with clearly visible structure to a continuous grafted area. By continuously varying the distance between the neighboring scans, the gradient distribution of the grafted molecules can be produced. Fluorescence signal for the structures produced at a lower end of the average laser power is weaker, indicating that the efficiency of the grafting process, i.e., the concentration of immobilized molecules depends on the irradiation dose. Figure 4b shows a scan through a woodpile pattern with a period of 25 µm. This structure allows to deduce that the lateral resolution produced by a single scan is about 4 µm. A rotated view of a single woodpile in Fig. 4c demonstrates the 3D capability of the developed multiphoton grafting method.

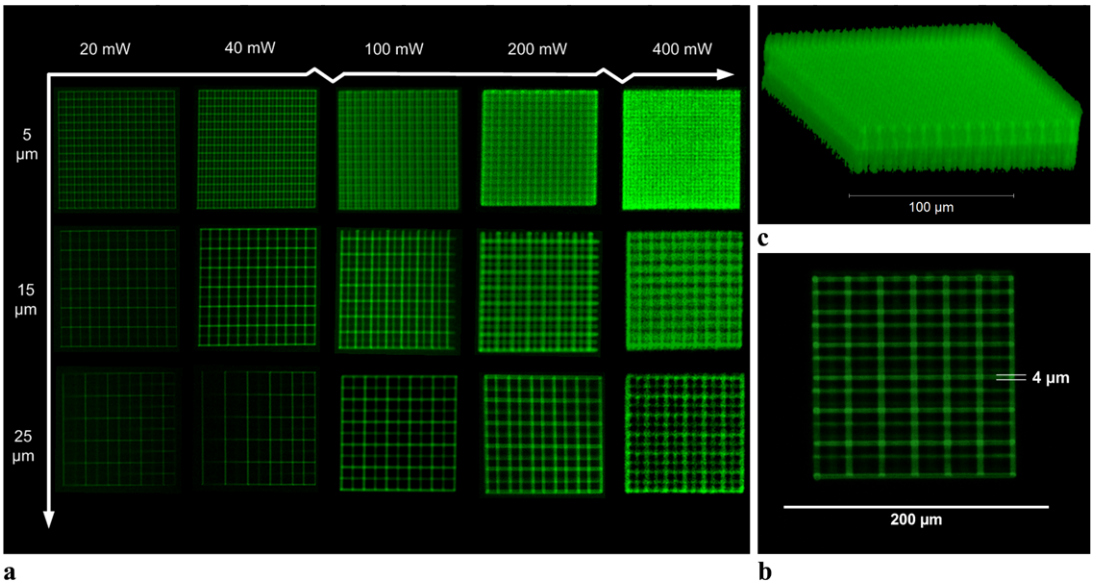

Fig. 4 Laser scanning microscopy images of patterns produced by three-photon grafting: (**a**) an overview of an array of woodpiles produced with different parameters; (**b**) fluorescent image of a scan through a woodpile pattern, showing the lateral resolution of around 4 µm; (**c**) a side view on a woodpile produced at an average power of 40 mW with a line distance of 5 µm

With regard to applications for bioactive surfaces, it should be noted that the achieved feature size is substantially smaller than the dimensions of most mammalian cells, while the entire pattern can be designed to cover the area/volume corresponding to the size of a single or multiple cells. Therefore, multiphoton grafting is a suitable tool for realization of well-defined configurable matrices for studies of cell attachment and migration [18, 19]. Also, for sensing applications, the resolution achieved by presented method is sufficient and would allow to place multiple sensing patterns within the same device [20]. Nevertheless, the use of immersion oil optics and shorter wavelength laser will facilitate further reduction of produced feature size down to at least about 65 nm as already found in the field of two-photon induced photopolymerization [21].

4 Conclusions

Nonlinear nature of the multi-photon absorption process allows initiation of photochemical reactions in a highly confined volume at a precise position within the sample. Here we have demonstrated true 3D functionalization of PEG-based matrices via photografting induced by three-photon absorption (3PA). The laser beam was focused by a conventional 20× microscope objective, yielding a lateral resolution of 4 µm. The use of aromatic azides facilitates applicability of the developed 3D grafting method to any polymeric matrices containing C–H or N–H bonds.

Furthermore, the nonlinear absorption properties of applied aromatic azide compound were thoroughly characterized by open aperture Z-scan method. Our findings indicate that photolysis induced by the 3PA is the enabling mechanism of demonstrated laser photografting. A value of 1.19×10^{-78} $cm^6\,s^2$ for the 3PA cross-section was derived from the obtained Z-scan data. This value is in good agreement with the one reported recently for a similar compound.

Presented results demonstrate the great potential of developed three-photon grafting method for precise 3D site-specific functionalization. To our best knowledge, this is the first report utilizing aromatic azide compounds for multi-photon induced grafting.

Acknowledgements The financial support by the China Scholarship Council (CSC) and Austrian Research Agency FFG under contract 819718 (ISOTEC) is greatly acknowledged. We would like to thank Dipl.-Ing. Enrico Dall'Ara for his technical assistance on the LSM.

References

1. C. Henneuse-Boxus, E. Dulière, J. Marchand-Brynaert, Eur. Polym. J. **37**, 9–18 (2001). doi:10.1016/S0014-3057(00)00094-X
2. A.J. Gross, S.S.C. Yu, A.J. Downard, Langmuir **26**, 7285–7292 (2010). doi:10.1021/la904442u
3. Y.S. Park, J. Won, Y.S. Kang, Langmuir **16**, 9662–9665 (2000). doi:10.1021/la000466v
4. R. Revanur, B. McCloskey, K. Breitenkamp, B.D. Freeman, T. Emrick, Macromolecules **40**, 3624–3630 (2007). doi:10.1021/ma0701033
5. C. Costas, Nucleic Acids Res. **28**, 1849–1858 (2000). doi:10.1093/nar/28.9.1849
6. A. Ovsianikov, V. Mironov, J. Stampfl, R. Liska, Expert Rev. Med. Devices (2012), accepted

7. S. Maruo, J.T. Fourkas, Laser Photonics Rev. **2**, 100–111 (2008). doi:10.1002/lpor.200710039
8. M. Rumi, S. Barlow, J. Wang, J.W. Perry, S.R. Marder, in *Photoresponsive Polymers I*, ed. by S.R. Marder, K.-S. Lee (Springer, Berlin, 2008), pp. 1–95. doi:10.1007/12_2008_133
9. H. Misawa, S. Juodkazis, *3D Laser Microfabrication: Principles and Applications* (Wiley-VCH, Weinheim, 2006). ISBN:9783527310555
10. B.H. Cumpston, S.P. Ananthavel, S. Barlow, D.L. Dyer, J.E. Ehrlich, L.L. Erskine, A.A. Heikal, S.M. Kuebler, I.-Y.S. Lee, D. McCord-Maughon, J. Qin, H. Rockel, M. Rumi, X.-L. Wu, S.R. Marder, J.W. Perry, Nature **398**, 51–54 (1999). doi:10.1038/17989
11. N. Pucher, A. Rosspeintner, V. Satzinger, V. Schmidt, G. Gescheidt, J. Stampfl, R. Liska, Macromolecules **42**, 6519–6528 (2009). doi:10.1021/ma9007785
12. M. Sheik-Bahae, A.A. Said, T.-H. Wei, D.J. Hagan, E.W. Van Stryland, IEEE J. Quantum Electron. **26**, 760–769 (1990). doi:10.1109/3.53394
13. B. Gu, W. Ji, H.-Z. Yang, H.-T. Wang, Appl. Phys. Lett. **96**, 081104 (2010). doi:10.1063/1.3327340
14. B. Gu, X.-Q. Huang, S.-Q. Tan, M. Wang, W. Ji, Appl. Phys. B **95**, 375–381 (2009). doi:10.1007/s00340-009-3426-y
15. J.M. Eisenhart, A.B. Ellis, J. Org. Chem. **50**, 4108–4113 (1985). doi:10.1021/jo00221a028
16. U. Gubler, C. Bosshard, Polymer **158**, 125–187 (2002). ISSN: 0032-3861
17. M.S. Hahn, J.S. Miller, J.L. West, Adv. Mater. **18**, 2679–2684 (2006). doi:10.1002/adma.200600647
18. N. Idota, T. Tsukahara, K. Sato, T. Okano, T. Kitamori, Biomaterials **30**, 2095–2101 (2009). doi:10.1016/j.biomaterials.2008.12.058
19. J.-F. Clemence, J.P. Ranieri, P. Aebischer, H. Sigrist, Bioconjug. Chem. **6**, 411–417 (1995). doi:10.1021/bc00034a011
20. L.K. Fiddes, H.K.C. Chan, B. Lau, E. Kumacheva, A.R. Wheeler, Biomaterials **31**, 315–320 (2010). doi:10.1016/j.biomaterials.2009.09.040
21. W. Haske, V.W. Chen, J.M. Hales, W. Dong, S. Barlow, S.R. Marder, J.W. Perry, Opt. Express **15**, 3426 (2007). doi:10.1364/OE.15.003426